Hindawi Publishing Corporation
International Journal of Antennas and Propagation
Volume 2015, Article ID 846720, 6 pages
http://dx.doi.org/10.1155/2015/846720

Research Article

Transmit TACAN Bearing Information with a Circular Array

W. Mark Dorsey, Jeffrey O. Coleman, and William R. Pickles

Radar Division, Naval Research Laboratory, Washington, DC 20375, USA

Correspondence should be addressed to W. Mark Dorsey; mark.dorsey@nrl.navy.mil

Received 6 August 2015; Accepted 30 September 2015

Academic Editor: Toni Björninen

Using TACAN and array fundamentals, we derive an architecture for transmitting TACAN bearing information from a circular array with time-varying weights. We evaluate performance for a simulated example array of Vivaldi elements.

1. Introduction

The Tactical Air Navigational (TACAN) system provides distance and bearing information to aircraft from ground stations and is widely used in military settings. Traditionally, a ground station's physically rotating transmit antenna creates bearing-dependent amplitude modulation from which aircraft can determine their bearings from that ground station. Where space for such a dedicated, special-purpose transmit antenna is difficult to obtain, such as on Naval vessels, sharing a multifunction array with other systems is an option. In that case the TACAN application would use time-varying array weights to approximate a rotating pattern.

Replacing the rotating antenna with a circular array would have benefits beyond facilitating the consolidation of apertures. Certainly these would include simplified maintenance [1] and the potential for elevation beam shaping and/or operation only within desired azimuth ranges [2]. In addition, an array could be given an operational bandwidth covering not only the current TACAN bands of 962–1024 MHz and 1025–1087 MHz [3] but also future TACAN bands considered likely to result from revised spectrum allocations [4].

With those motivations, this paper derives time-varying TACAN array weights for a uniform cylindrical array. While TACAN specifications [5] address both the static elevation pattern and the dynamic azimuth pattern, here we focus on the latter. Our design example assumes an array of Vivaldi elements characterized by embedded element patterns obtained through HFSS simulations. To evaluate the design, we use a bearing-error metric that falls naturally out of the derivation.

The standard TACAN ground transmitter of interest slowly amplitude-modulates a fast pulse signal with an antenna pattern that rotates at 15 Hz and that is designed to yield sinusoidal AM components, in the pulse amplitudes at the aircraft receiver, at 15 Hz and $9 \times 15\,\text{Hz} = 135\,\text{Hz}$. A reference burst transmitted as the rotating main lobe passes north enables an aircraft to obtain a coarse bearing from the transmitter as the phase of the 15 Hz modulation component relative to a zero time marked by burst reception. That coarse bearing and the phase of the 135 Hz component then together yield a fine bearing measurement. Here we focus on creating a time-varying array pattern that permits accurate bearing estimation at the receiver using this process. The fast pulse modulation and reference bursts are independent of the antenna and pattern used and are not considered further here.

This paper presents the initial study into the development of the time-harmonic weights required for transmitting the TACAN waveform from a circular array. A discussion on the theory is provided and validated using simulations.

2. Theory

The next section derives the array structure and time-varying array weights. Performance is then derived as a function of those weights and the complex embedded array patterns.

2.1. Deriving the Array. Time-varying weights for a circular array of N elements are derived below with the goal of providing accurate TACAN bearing measurement in receivers at arbitrary bearings.

There are several steps. Formally assuming the array to be circularly symmetric and requiring its pattern sampled at N equally spaced bearings to smoothly rotate in space with time turns out—no surprise—to formally imply that the weights must also rotate so that only one weight requires explicit design. That design follows from the desired temporal modulation of the array-pattern amplitude along a single direction. The pattern modulation between the N bearings thus addressed explicitly takes the desired general form automatically, with only pattern magnitude and signal modulation indices free to vary modestly (given reasonable assumptions) with bearing.

2.1.1. The Array. Center the N-element array on the origin with symmetry about the vertical axis and with element indices increasing with bearing. Align element 0 with bearing 0° (any bearing can be made the new zero by changing the reference-burst timing) and interpret element indices modulo N so that the elements adjacent to element 0, for example, can be indexed with ± 1 or $\{1, N-1\}$. In the development below, each summation $\sum$ over index n should be read as a sum over element indices $n = 0, \ldots, N-1$, and each summation $\sum$ over index ℓ should be read as the doubly infinite sum over $\ell = -\infty, \ldots, \infty$.

Let $\mathbf{k}$ designate the real wavenumber vector of a transmitted signal, and let complex vector-valued function $\vec{f}_n(\mathbf{k})$ be the origin-referenced embedded far-field complex pattern of element n. We assume elements are identical in the sense that

$$\vec{f}_n(\mathbf{k}) = \mathbf{R}^n \vec{f}_0\left(\mathbf{R}^{-n}\mathbf{k}\right) \tag{1}$$

for all $\mathbf{k}$ of interest, where linear operation $\mathbf{v} \mapsto \mathbf{R}\mathbf{v}$ rotates real vector $\mathbf{v}$ about the vertical by $2\pi/N$ to increase bearing. Identity $\mathbf{R}^N = \mathbf{R}$ will be used freely.

In practice imperfect array construction will result in nonidentical embedded element patterns, so the transmitted TACAN waveform will vary somewhat from the ideal derived here. We have yet to study such errors but hope to eventually.

2.1.2. One Weight Implies the Others. Write the time-varying far-field complex array pattern as

$$\vec{f}(\mathbf{k}, t) = \sum_n w_n(t)\, \vec{f}_n(\mathbf{k}) = \sum_n w_n(t)\, \mathbf{R}^n \vec{f}_0\left(\mathbf{R}^{-n}\mathbf{k}\right) \tag{2}$$

using array symmetry (1) on the right. A classic TACAN system's pattern rotates spatially at frequency $1/T = 15\,\text{Hz}$, but here we require that behavior only at N equally spaced bearings. Period T rotation over $2\pi/N$ in angle is given by

$$\vec{f}(\mathbf{R}\mathbf{k}, t) = \mathbf{R}\vec{f}\left(\mathbf{k}, t - \frac{T}{N}\right). \tag{3}$$

Substituting $\mathbf{R}\mathbf{k}$ for $\mathbf{k}$ in (2) and a change of index yield

$$\vec{f}(\mathbf{R}\mathbf{k}, t) = \sum_n w_n(t)\, \mathbf{R}^n \vec{f}_0\left(\mathbf{R}^{1-n}\mathbf{k}\right), \tag{4}$$

$$\vec{f}(\mathbf{R}\mathbf{k}, t) = \sum_n w_{n+1}(t)\, \mathbf{R}^{n+1} \vec{f}_0\left(\mathbf{R}^{-n}\mathbf{k}\right). \tag{5}$$

Likewise, applying (2) to the right side of (3) yields

$$\mathbf{R}\vec{f}\left(\mathbf{k}, t - \frac{T}{N}\right) = \sum_n w_n\left(t - \frac{T}{N}\right) \mathbf{R}^{n+1} \vec{f}_0\left(\mathbf{R}^{-n}\mathbf{k}\right). \tag{6}$$

Substituting (5) and (6) into (3) and comparing terms then formally show that $w_{n+1}(t) = w_n(t - T/N)$ for all n, so

$$w_n(t) = w_0\left(t - \frac{nT}{N}\right). \tag{7}$$

A rotating bearing-sampled pattern thus implies weight periodicity $w_0(t) = w_N(t) = w_0(t - T)$. This will not produce rotation for all bearings, but we will preserve property (7) for simplicity of structure and in order to obtain nearly rotating behavior.

2.1.3. Desired Modulation. The desired complex array pattern is an arbitrary constant complex amplitude modulated by

$$\begin{aligned} m(t, \phi) = 1 &+ 2a\cos\left(\frac{2\pi t}{T} - \phi\right) \\ &+ 2b\cos\left(\frac{2\pi 9t}{T} - 9\phi\right), \end{aligned} \tag{8}$$

where ϕ is bearing. Positive real modulation indices $2a$ and $2b$ are kept small enough that $|m(t, \phi)| = m(t, \phi)$, for simple receiver demodulation. The terms at frequencies $1/T$ and $9/T$ are, respectively, used for coarse and fine bearing measurement.

The $\phi = 0$ array pattern should be, using arbitrary scaling,

$$m(t, 0) = 1 + 2a\cos\left(\frac{2\pi t}{T}\right) + 2b\cos\left(\frac{2\pi 9t}{T}\right). \tag{9}$$

2.1.4. Determining Weight $w_0(t)$. Let wavenumber vector $\mathbf{k}_{\text{imp}}$ and complex polarization unit vector $\vec{c}$ govern co-pol propagation at $\phi = 0$ at the most important elevation. Using superscripts to index coefficients, the Fourier series of associated pattern sample $\langle \vec{f}(\mathbf{k}_{\text{imp}}, t), \vec{c}\rangle$ and weight $w_0(t)$ take forms

$$\left\langle \vec{f}\left(\mathbf{k}_{\text{imp}}, t\right), \vec{c}\right\rangle = \sum_\ell c^\ell \mathrm{e}^{j2\pi\ell t/T}, \tag{10}$$

$$w_0(t) = \sum_\ell w^\ell \mathrm{e}^{j2\pi\ell t/T}. \tag{11}$$

The co-pol array pattern at $\mathbf{k} = \mathbf{k}_{\text{imp}}$ is, by (2) and (7),

$$\left\langle \vec{f}\left(\mathbf{k}_{\text{imp}}, t\right), \vec{c}\right\rangle = \sum_n \left\langle \vec{f}_n\left(\mathbf{k}_{\text{imp}}\right), \vec{c}\right\rangle w_0\left(t - \frac{nT}{N}\right). \tag{12}$$

Fourier-series forms (10) and (11) and simple algebra then yield

$$\sum_\ell c^\ell \mathrm{e}^{j2\pi\ell t/T} = \sum_\ell w^\ell h^\ell \mathrm{e}^{j2\pi\ell t/T} \tag{13}$$

after defining DFT sum (periodically extended in ℓ)

$$h^\ell = \sum_n \left\langle \vec{f}_n\left(\mathbf{k}_{\text{imp}}\right), \vec{c}\right\rangle \mathrm{e}^{-j2\pi\ell n/N}, \tag{14}$$

which allows h^ℓ to be computed from the embedded complex element patterns. The $\phi = 0$ pattern (9)

$$\begin{aligned}\left\langle \vec{f}\left(\mathbf{k}_{\text{imp}}, t\right), \vec{c}\right\rangle &= m(t,0)\\ &= 1 + ae^{j2\pi t/T} + ae^{-j2\pi t/T} + be^{j2\pi 9t/T}\\ &\quad + be^{-j2\pi 9t/T}\end{aligned} \tag{15}$$

yields coefficients c^ℓ. From these h^ℓ and c^ℓ we can obtain w^ℓ using the uniqueness of Fourier series and (13), which imply

$$c^\ell = w^\ell h^\ell \tag{16}$$

for integer ℓ. Thus Fourier series (11) can be written as

$$\begin{aligned}w_0(t) = \frac{1}{h^0} + \frac{a}{h^1}e^{j2\pi t/T} + \frac{a}{h^{-1}}e^{-j2\pi t/T} + \frac{b}{h^9}e^{j2\pi 9t/T}\\ + \frac{b}{h^{-9}}e^{-j2\pi 9t/T}.\end{aligned} \tag{17}$$

This and (7) specify weights that fix the co-pol array pattern for the N wavenumber vectors of form $\mathbf{R}^n\mathbf{k}_{\text{imp}}$ to ideal values. The pattern in other directions/polarizations cannot be independently specified and depends on the element patterns.

2.2. Performance

2.2.1. The Received Signal's Overall Amplitude Modulation. Much of the above can be generalized to arbitrary polarization unit vector $\vec{p}$ and wavenumber vector $\mathbf{k}$. Generalizing Fourier series (10) along with (13) and (14),

$$\left\langle \vec{f}(\mathbf{k}, t), \vec{p}\right\rangle = \sum_\ell p^\ell e^{j2\pi\ell t/T}, \tag{18}$$

$$p^\ell = w^\ell \sum_n \left\langle \vec{f}_n(\mathbf{k}), \vec{p}\right\rangle e^{-j2\pi\ell n/N}. \tag{19}$$

Using (17) for w^ℓ, the nonzero Fourier coefficients are

$$\begin{aligned}p^0 &= \frac{1}{h^0}\sum_n \left\langle \vec{f}_n(\mathbf{k}), \vec{p}\right\rangle,\\ p^{\pm 1} &= \frac{a}{h^{\pm 1}}\sum_n \left\langle \vec{f}_n(\mathbf{k}), \vec{p}\right\rangle e^{\mp j2\pi n/N},\\ p^{\pm 9} &= \frac{b}{h^{\pm 9}}\sum_n \left\langle \vec{f}_n(\mathbf{k}), \vec{p}\right\rangle e^{\mp j2\pi 9n/N}.\end{aligned} \tag{20}$$

Fourier sum (18) is a complex constant times a real modulation function if each of $p^{\pm 1}/p^0$ and $p^{\pm 9}/p^0$ is a conjugate pair. To distinguish desired and undesired pair behaviors, we can define sum and difference coefficients. For each $k \in \{1, 9\}$, let

$$\begin{aligned}p_{k\Sigma} &= \frac{p^k}{p^0} + \left(\frac{p^{-k}}{p^0}\right)^*,\\ p_{k\Delta} &= \frac{p^k}{p^0} - \left(\frac{p^{-k}}{p^0}\right)^*\end{aligned} \tag{21}$$

so that

$$\begin{aligned}\frac{p^k}{p^0} &= \frac{p_{k\Sigma} + p_{k\Delta}}{2},\\ \frac{p^{-k}}{p^0} &= \frac{\left(p_{k\Sigma} - p_{k\Delta}\right)^*}{2}.\end{aligned} \tag{22}$$

Fourier sum (18) then becomes

$$\begin{aligned}\left\langle \vec{f}(\mathbf{k}, t), \vec{p}\right\rangle = p^0\Big(1 + \frac{1}{2}\Big(&p_{1\Sigma}e^{j2\pi t/T} + p_{1\Sigma}^* e^{-j2\pi t/T}\\ &+ p_{1\Delta}e^{j2\pi t/T} - p_{1\Delta}^* e^{-j2\pi t/T} + p_{9\Sigma}e^{j2\pi 9t/T}\\ &+ p_{9\Sigma}^* e^{-j2\pi 9t/T} + p_{9\Delta}e^{j2\pi 9t/T} - p_{9\Delta}^* e^{-j2\pi 9t/T}\Big)\Big).\end{aligned} \tag{23}$$

Combining sums and differences of conjugate pairs yields

$$\begin{aligned}\left\langle \vec{f}(\mathbf{k}, t), \vec{p}\right\rangle = p^0\Big(1 &+ \mathrm{Re}\left\{p_{1\Sigma}e^{j2\pi t/T}\right\}\\ &+ \mathrm{Re}\left\{p_{9\Sigma}e^{j2\pi 9t/T}\right\} + j\,\mathrm{Im}\left\{p_{1\Delta}e^{j2\pi t/T}\right\}\\ &+ j\,\mathrm{Im}\left\{p_{9\Delta}e^{j2\pi 9t/T}\right\}\Big)\end{aligned} \tag{24}$$

or

$$\begin{aligned}\left\langle \vec{f}(\mathbf{k}, t), \vec{p}\right\rangle = p^0\Big(1 &+ \left|p_{1\Sigma}\right|\cos\left(\frac{2\pi t}{T} + \angle p_{1\Sigma}\right)\\ &+ \left|p_{9\Sigma}\right|\cos\left(\frac{2\pi 9t}{T} + \angle p_{9\Sigma}\right)\\ &+ j\left|p_{1\Delta}\right|\sin\left(\frac{2\pi t}{T} + \angle p_{1\Delta}\right)\\ &+ j\left|p_{9\Delta}\right|\sin\left(\frac{2\pi 9t}{T} + \angle p_{9\Delta}\right)\Big).\end{aligned} \tag{25}$$

Ideally $|p_{1\Delta}|$ and $|p_{9\Delta}|$ are negligibly small so that

$$\begin{aligned}\left|\left\langle \vec{f}(\mathbf{k}, t), \vec{p}\right\rangle\right| = \left|p^0\right|\Big|1 &+ \left|p_{1\Sigma}\right|\cos\left(\frac{2\pi t}{T} + \angle p_{1\Sigma}\right)\\ &+ \left|p_{9\Sigma}\right|\cos\left(\frac{2\pi 9t}{T} + \angle p_{9\Sigma}\right)\Big|.\end{aligned} \tag{26}$$

In analogy to (8), magnitudes $|p_{1\Sigma}|$ and $|p_{9\Sigma}|$ are the modulation indices, and angles

$$\angle p_{1\Sigma} \overset{\text{mod } 2\pi}{=} -\phi_{\text{coarse}}, \tag{27}$$

$$\angle p_{9\Sigma} \overset{\text{mod } 2\pi}{=} -9\phi_{\text{fine}} \tag{28}$$

relate to coarse and fine bearing estimates ϕ_{coarse} and ϕ_{fine}.

2.2.2. The Fine Bearing Measurement. The receiver can compute ϕ_{coarse} from (27) directly, but computing ϕ_{fine} requires resolving the ninefold ambiguity in (28). The key is to let

$$\phi_{\text{diff}} \overset{\text{mod } 2\pi}{=} \phi_{\text{fine}} - \phi_{\text{coarse}} \tag{29}$$

and assume that since ϕ_{coarse} and ϕ_{fine} are close as angles, $\phi_{\text{diff}} \in [-\pi/9, \pi/9)$. Scaling (29) by $9/2\pi$ and using (27) and (28),

$$\frac{9\phi_{\text{diff}}}{2\pi} + m = \frac{9\angle p_{1\Sigma} - \angle p_{9\Sigma}}{2\pi} \tag{30}$$

for some integer m. Since $9\phi_{\text{diff}}/2\pi \in [-1/2, 1/2)$, rounding yields the first of the three needed computational steps, and (30) and (29) yield the other two:

$$\begin{aligned} m &= \text{round}\left(\frac{9\angle p_{1\Sigma} - \angle p_{9\Sigma}}{2\pi}\right), \\ \phi_{\text{diff}} &= \angle p_{1\Sigma} - \frac{\angle p_{9\Sigma} + 2\pi m}{9}, \\ \phi_{\text{fine}} &= \left(\phi_{\text{coarse}} + \phi_{\text{diff}}\right) \bmod 2\pi. \end{aligned} \tag{31}$$

2.2.3. Intrinsic Bearing Measurement Error. The measured bearing generally contains some error even when $p_{1\Delta} = p_{9\Delta} = 0$ and when the receiver measures angles $\angle p_{1\Sigma}$ and $\angle p_{9\Sigma}$ perfectly. To derive the intrinsic residual fine bearing error relative to actual bearing ϕ, add 9ϕ to each side of (28) and apply angle-folding map $x \mapsto ((x+\pi) \bmod 2\pi) - \pi$. This yields $((\angle p_{9\Sigma} + 9\phi + \pi) \bmod 2\pi) - \pi = -9(\phi_{\text{fine}} - \phi)$, where the right side is unchanged because the map is an identity when $-\pi \le x < \pi$. The intrinsic fine bearing error is therefore

$$\phi_{\text{fine}} - \phi = \frac{\left(\pi - \left(\left(\angle p_{9\Sigma} + 9\phi + \pi\right) \bmod 2\pi\right)\right)}{9}. \tag{32}$$

Replace 9 by unity to derive intrinsic coarse bearing error

$$\phi_{\text{coarse}} - \phi = \left(\pi - \left(\left(\angle p_{1\Sigma} + \phi + \pi\right) \bmod 2\pi\right)\right). \tag{33}$$

3. Simulation

We tested the approach using weights and performance measures computed from simulated vertical-polarization element patterns $\langle \vec{f}_n(\mathbf{k}), \vec{c} \rangle$ of 45 Vivaldi radiators embedded in the uniform circular array of Figure 1. The 1 GHz carrier frequency and 22.9 cm (11.0 in) array radius used were convenient but have no TACAN significance. HFSS array simulation with one element driven and the others terminated yielded one embedded element pattern, and (1) provided the rest. Time-varying array excitations are from (7) and (17). We aimed wavenumber vector $\mathbf{k}_{\text{imp}}$ at the north horizon for a zero "most important elevation." Modulation indices $2a$ and $2b$ were each set to 0.2 per Shestag [2].

The embedded co-pol element pattern $\langle \vec{f}_n(\mathbf{k}), \vec{c} \rangle$ of the Vivaldi radiator appears in Figure 2. Essentially all of the samples used in DFT (14) were significant in magnitude.

Figure 3 shows that the co-pol array pattern obtained approximates 15 Hz rotation, and the Figure 4 slice at $t = 0$ of that pattern hews closely to desired form (8) from Shestag [2]. In both figures, gain is normalized to the $t = 0$ peak.

Section 2.2 discussion assumed that, for $n \in \{1, 9\}$, the hypotenuse of a right triangle with side lengths $|p_{n\Delta}|$ and $|p_{n\Sigma}|$ was essentially of the latter length because $|p_{n\Delta}|$ was relatively tiny. This is verified in Figure 5.

Figure 6 shows that time-average array gain $20\log_{10}|p^0|$ and modulation indices $|p_{1\Sigma}|$ and $|p_{9\Sigma}|$ vary little with bearing. Average gain is consistent with Figure 4, and the modulation indices approximate the 20% desired value.

The most important quantities computed in this system simulation are undoubtedly the intrinsic errors (32) and (33) in the coarse and fine bearing measurements, respectively,

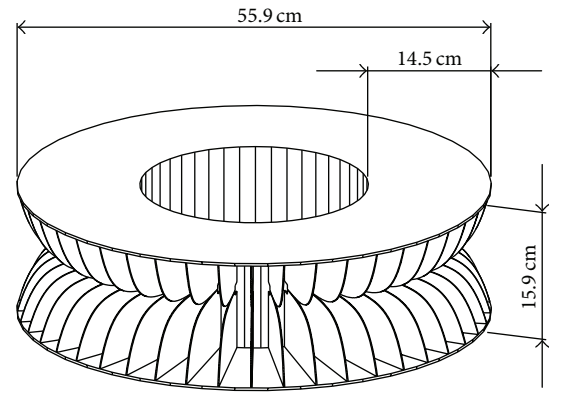

Figure 1: Simulated uniform circular array of 45 Vivaldi radiators.

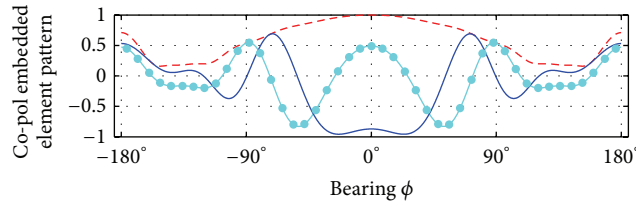

Figure 2: Real (solid) and imaginary (knobby) parts and magnitude (dashed) of embedded co-pol pattern $\langle \vec{f}_0(\mathbf{k}), \vec{c} \rangle$ of element zero, on a linear scale, with $\mathbf{k}$ at bearing ϕ and the elevation of $\mathbf{k}_{\text{imp}}$. The elements are identical, so the knobs every 8° mark those ϕ where the curves also yield the $\langle \vec{f}_n(\mathbf{k}_{\text{imp}}), \vec{c} \rangle$ for $n = 0, \ldots, N-1$ used in DFT (14).

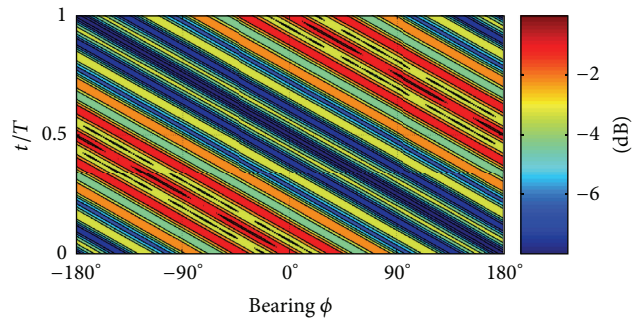

Figure 3: Co-pol array gain as a function of bearing and time over period $T = 1/(15\,\text{Hz})$.

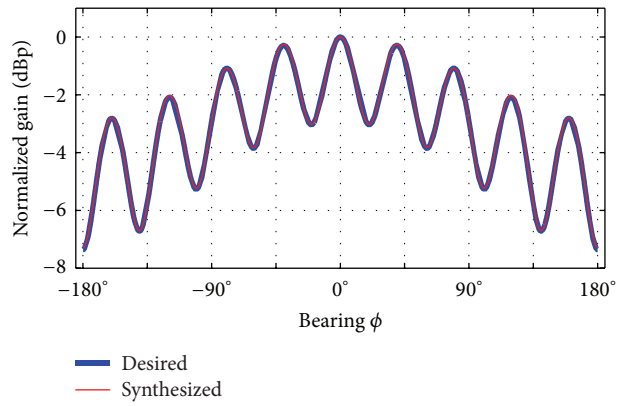

FIGURE 4: This paper's synthesized $t = 0$ co-pol array gain plotted over the desired pattern of (8) and [2].

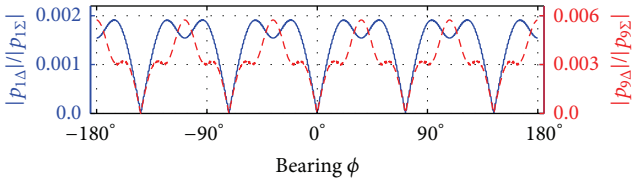

FIGURE 5: Approximating (25) by (26) is validated by the small error ratio $|p_{n\Delta}|/|p_{n\Sigma}|$ shown here for $n = 1$ (solid curve) and $n = 9$ (dashed curve).

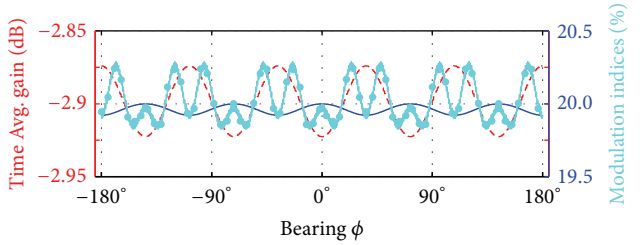

FIGURE 6: Time-averaged co-pol array gain (dashed curve using same normalization as Figures 3 and 4) and modulation indices for the 15 Hz (solid curve) and 135 Hz (knobby curve) components of the AM signal.

intrinsic because they assume noise-free reception at the aircraft. Those are shown in Figure 7. The intrinsic errors in the fine bearing measurement never exceed 0.1° in magnitude, while the magnitudes of the coarse errors never exceed 0.02°. While this appears to suggest that coarse measurement is more accurate, this is somewhat illusory, as the error component due to signal noise, not included here, will generally dominate and be substantially greater for the coarse measurement than for the fine measurement. Certainly the Figure 7 numbers leave plenty of room for those noise-related errors before the TACAN system error limits of 10° and 2° for the coarse and fine readings, respectively [5], are breached.

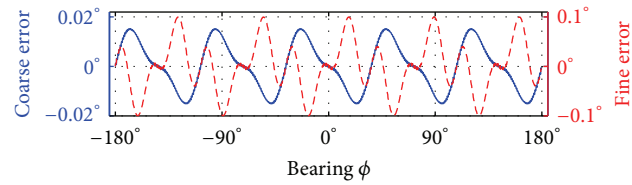

FIGURE 7: Bearing measurement errors computed from the phases of $p_{1\Sigma}$ and $p_{9\Sigma}$ for coarse (solid curve) and fine (dashed curve) bearing information, respectively.

4. Conclusions

In this preliminary study, we developed time-harmonic weights to allow a uniform circular array to support TACAN transmission of bearing information. We have shown how those time-varying weights can be determined from the embedded element pattern. Design and error calculations for an example circular array of Vivaldi elements suggest that acceptable accuracy is feasible with reasonable arrays.

Appropriate future work to expand upon these beginnings includes examining performance over an appropriate elevation interval, considering other array dimensions and numbers of elements, exploring other element geometries, and, of course, validating the theoretical development via measurements. Probably most important, however, is to explore the effects of imperfect knowledge of the embedded element patterns.

Disclosure

Jeffrey O. Coleman collaborated with former colleagues at the Naval Research Laboratory for this work; he has actually retired from that laboratory.

Conflict of Interests

The authors declare that there is no conflict of interests regarding the publication of this paper.

Acknowledgment

This work is supported by the InTop program of the Office of Naval Research.

References

[1] E. J. Christopher, "Electronically scanned TACAN antenna," *IEEE Transactions on Antennas and Propagation*, vol. 22, no. 1, pp. 12–16, 1974.

[2] L. N. Shestag, "A cylindrical array for the TACAN system," *IEEE Transactions on Antennas and Propagation*, vol. 22, no. 1, pp. 17–25, 1974.

[3] A. Casabona, "Antenna for the AN/URN-3 Tacan beacon," *Electrical Communications*, vol. 33, pp. 35–59, 1956.

[4] G. W. Hein, J.-A. Avila-Rodriguez, S. Wallner, B. Eissfeller, M. Irsigler, and J.-L. Issler, "A vision on new frequencies, signals and

concepts for future GNSS systems," in *Proceedings of the 20th International Technical Meeting of the Satellite Division of the Institute of Navigation (ION GNSS '07)*, pp. 517–534, Fort Worth, Tex, USA, September 2007.

[5] S. J. Foti, M. W. Shelley, R. Cahill et al., "An intelligent electronically spinning TACAN antenna," in *Proceedings of the 19th European Microwave Conference*, pp. 959–965, IEEE, London, UK, September 1989.